Finsler Geodesics Evolution Model for Region-Based Active Contours

Da Chen[1]
chenda@ceremade.dauphine.fr

Jean-Marie Mirebeau[2]
jean-marie.mirebeau@math.u-psud.fr

Laurent D. Cohen[1]
cohen@ceremade.dauphine.fr

[1] CEREMADE, CNRS, University Paris Dauphine, PSL Research University, UMR 7534, 75016 PARIS, FRANCE

[2] Laboratoire de mathématiques d'Orsay, CNRS, Université Paris-Sud, Université Paris-Saclay, 91405 ORSAY, FRANCE

Abstract

In this paper, we introduce a new deformable model for image segmentation, by reformulating a region-based active contours energy into a geodesic contour energy involving an asymmetric Finsler metric. As a consequence, we solve the region-based active contours energy minimization problem without resorting to level set functions, but using a robust Eikonal equation framework. By sampling a set of control points from the closed active contour in clockwise order, the active contours evolution problem is turned into finding a collection of minimal curves joining all the ordered control points. Therefore, the proposed model can blend the benefits of the curve evolution scheme and the Eikonal equation-based minimal path technique. Globally optimal minimal curves are obtained by solving an Eikonal equation, involving a Finsler metric, which is achieved at a modest numerical cost using a variant of the fast marching algorithm.

1 Introduction

The class of active contours methods, addressing image segmentation problems using adequate curve evolution models, has attracted vast attention since the pioneer work of Kass *et al.* [19]. These active contours models treat object boundaries as closed curves that minimize the corresponding energy functionals, invoking either region information [10, 21, 26, 30, 31] or edge information [9, 15, 19, 32, 33].

The energy functionals of region-based active contours models consider the similarity measurement of gray levels, colors or textures inside each region component. Mumford and Shah [26] presented a model using a piecewise smooth function to approximate the image intensities. Later on, it was shown that the Mumford-Shah functional can be minimized by curve evolution schemes [30, 31], in which the curves are represented by the zero values of level set functions [27]. Chan and Vese [10] consider a reduced form of Mumford-Shah functional based on the variation level set framework [34]. In [10], the authors approximated the image intensities by two constants, which is relevant to the cartoon model as discussed in [26]. The basic idea of the local region-based models [20, 21] is to consider a scale function in their energy functionals to deal with the intensities inhomogeneity problem.

Other interesting region-based active contours models include the pairwise similarity energy functional models [6, 17, 18, 29].

Edge-based active contours models often regard the image gradient inverse magnitude as a potential function, so as to attract the contours toward the expected boundaries. An important shortcoming of these models is that they are sensitive to the local minimas of the respective energies. Sometimes the contours will be trapped to spurious edges produced by noise. Eikonal PDE-based minimal path model was introduced by Cohen and Kimmel [16] to solve the initialization and minimization problems suffered by the classical snakes model [19]. This minimal path model can efficiently find the global minimum of the isotropic Riemannian metric-based geodesic energy [9] between two points thanks to Eikonal interpretation and the fast marching algorithm [28]. Recent improvements to the minimal path model focus on the orientation [5, 7] and curvature [3, 14] enhancement. Applications of the minimal path models also have been deeply studied in the last two decades [1, 2, 4, 12, 13]. Mille *et al.* [24] proposed a minimal paths-based model for interactive image segmentation, relying on a set of admissible paths by the concept of saddle point in terms of image edge information. Then a region, edge, and contour simplicity based hybrid energy was constructed. An optimal combination of paths from the admissible paths set was chosen to minimize the hybrid energy in a manner of greedy.

Finsler metric-based geodesic active contours model was introduced by Melonakos *et al.* [23] for image segmentation and tubular structure extraction. This Finsler metric-based model extends the isotropic Riemannian metric [9, 16] to the asymmetric and anisotropic case, thus defining a general geodesic energy that takes into account the curve orientation information.

In this paper, we present a new Finsler geodesics evolution model for region-based image segmentation. We build the connection between the Eikonal equation-based minimal path model and the region-based active contours models via a Finsler metric. The minimal paths in our model can be determined by pure region information or by both region and edge information. The initialization is also flexible: one can provide a contour or a set of points distributed on the object boundaries.

2 Region-Based Active Contours Models and Finsler Minimal Path Model

2.1 Mumford-Shah Functional based Active Contours Models

The classical Mumford-Shah (MS) functional [26] combines region-based term and a curve length regularization term

$$E^{\mathrm{MS}}(g,\gamma) = \alpha \int_{\Omega} (I(\mathbf{x}) - g(\mathbf{x}))^2 \, d\mathbf{x} + \beta \int_{\Omega \setminus \gamma} \|\nabla g(\mathbf{x})\|^2 d\mathbf{x} + \lambda \int_0^1 \|\dot{\gamma}(t)\| dt, \qquad (1)$$

where $\Omega \subset \mathbb{R}^2$ is the image domain and $I : \Omega \to \mathbb{R}$ is an observed gray level image. g is a piecewise smooth image data function used to approximate I inside each region component and $\gamma : [0,1] \to \Omega$ is a smooth curve. α, β and λ are positive constants. It is known that minimizing the original MS functional E^{MS} is a difficult task. Vese and Chan [31] and Tasi *et al.* [30] independently proposed numerical approaches to the original MS problem based on active contours evolution. Along the same research line, Brox and Cremers [8] statistically interpreted the piecewise smooth MS functional by a local region-based model.

Chan-Vese (CV) Piecewise Constant Active Contours Model: Chan and Vese [11] presented a region-based active contours model where the energy functional is obtained from the reduced form of the original MS functional by setting the piecewise smooth function g to be constants c_1 inside γ and to be c_2 outside γ. In its basic formulation, the contour γ was represented by the zero-value of the level set function Φ [27]. By a variational level set approach [34] invoking a Heaviside function $H : \Omega \to \{0, 1\}$, the variational level set-based CV model functional [11] can be expressed as

$$E^{\text{CV}}(\Phi, c_1, c_2) = \alpha_1 \int_\Omega (I(\mathbf{x}) - c_1)^2 H(\Phi(\mathbf{x})) d\mathbf{x} + \alpha_2 \int_\Omega (I(\mathbf{x}) - c_2)^2 H(-\Phi(\mathbf{x})) d\mathbf{x}$$
$$+ \lambda \int_\Omega \|\nabla H(\Phi(\mathbf{x}))\| d\mathbf{x} + \nu \int_\Omega H(\Phi(\mathbf{x})) d\mathbf{x}, \tag{2}$$

where the last term of above energy functional is an optional ballon force [15].

Local Binary Fitting (LBF) Model: The LBF model [21] was introduced by Li *et al.*to deal with inhomogeneous intensities problem. This model introduced a local gaussian kernel to the active contours energy in the variational level set form:

$$E^{\text{LBF}}(\Phi, u_1, u_2) = \int_\Omega \mathcal{J}_{\mathbf{x}}(\Phi, u_1, u_2) d\mathbf{x}, \tag{3}$$

where one has

$$\mathcal{J}_{\mathbf{x}}(\Phi, u_1, u_2) = \int_\Omega G_\sigma(\mathbf{y} - \mathbf{x}) \Big((I(\mathbf{y}) - u_1(\mathbf{x}))^2 H(\Phi(\mathbf{y})) + (I(\mathbf{y}) - u_2(\mathbf{x}))^2 H(-\Phi(\mathbf{y})) \Big) d\mathbf{y}.$$

2.2 Eikonal Equation-based Minimal Path Model

Classical Minimal Path Model: The Eikonal equation-based minimal path model was introduced by Cohen and Kimmel [16] to globally minimize the geodesic energy between two points:

$$\ell(\gamma) = \int_0^1 P(\gamma(t)) \|\dot{\gamma}(t)\| dt, \tag{4}$$

where P is a potential function. Denote by $\mathcal{U}(\mathbf{x}) = \sup_{\gamma \in \mathcal{A}} \{\ell(\gamma); \gamma(0) = \mathbf{s}, \gamma(1) = \mathbf{x}\}$ the global minimum of ℓ among the set $\mathcal{A}$ of admissible paths joining a fixed source point $\mathbf{s}$ to the target $\mathbf{x}$. It is well known that $\mathcal{U}$ satisfies the Eikonal equation [16]:

$$\|\nabla \mathcal{U}(\mathbf{x})\| = P(\mathbf{x}), \quad \forall \mathbf{x} \in \Omega \backslash \{\mathbf{s}\}, \quad \text{and } \mathcal{U}(\mathbf{s}) = 0. \tag{5}$$

Once the minimal action map $\mathcal{U}$ is obtained by the fast marching algorithm [28], one can track the minimal geodesic from the source point $\mathbf{s}$ to the target $\mathbf{x}$ by solving the ODE:

$$\dot{\mathcal{C}}_{\mathbf{s},\mathbf{x}}(t) \propto \nabla \mathcal{U}(\mathcal{C}_{\mathbf{s},\mathbf{x}}(t)), \quad \text{with } \mathcal{C}_{\mathbf{s},\mathbf{x}}(0) = \mathbf{s}. \tag{6}$$

Finsler Minimal Path Model: We consider a Finsler metric $\mathcal{P} : \Omega \times \mathbb{R}^2 \to \mathbb{R}^+$ with the form of

$$\mathcal{P}(\mathbf{x}, \mathbf{u}) = P(\mathbf{x}) \|\mathbf{u}\| - \langle \omega(\mathbf{x}), \mathbf{u} \rangle, \quad \forall \mathbf{x} \in \Omega, \forall \mathbf{u} \in \mathbb{R}^2, \tag{7}$$

which obeys a smallness condition [14, 25]

$$\|\omega(\mathbf{x})\| < P(\mathbf{x}), \quad \forall \mathbf{x} \in \Omega, \tag{8}$$

ensuring that $\mathcal{P}(\mathbf{x}, \mathbf{u})$ will be always positive for all $\mathbf{x} \in \Omega$ and any nonzero vector $\mathbf{u} \in \mathbb{R}^2$. The Eikonal equation associated to this Finsler metric $\mathcal{P}$ is [14, 25]

$$\begin{cases} \mathcal{P}^*(\mathbf{x}, \nabla \mathcal{U}(\mathbf{x})) = 1, & \forall \mathbf{x} \in \Omega \backslash \{\mathbf{s}\}, \\ \mathcal{U}(\mathbf{s}) = 0, \end{cases} \tag{9}$$

where $\mathcal{P}^*$ is the dual metric of $\mathcal{P}$ defined by

$$\mathcal{P}^*(\mathbf{x}, \mathbf{u}) = \sup_{\mathbf{v} \neq \mathbf{0}} \frac{\langle \mathbf{u}, \mathbf{v} \rangle}{\mathcal{P}(\mathbf{x}, \mathbf{v})}.$$

The geodesic $\mathcal{C}_{\mathbf{s},\mathbf{x}}$ joining $\mathbf{s}$ to $\mathbf{x}$, with respect to the metric $\mathcal{P}$, can be tracked by solving

$$\dot{\mathcal{C}}_{\mathbf{s},\mathbf{x}}(t) \propto -\nabla \mathcal{P}^*\left(\mathcal{C}_{\mathbf{s},\mathbf{x}}(t), \nabla \mathcal{U}(\mathcal{C}_{\mathbf{s},\mathbf{x}}(t))\right), \quad \text{and} \quad \mathcal{C}_{\mathbf{s},\mathbf{x}}(0) = \mathbf{s}. \tag{10}$$

3 Finsler Geodesics Evolution Model

3.1 Region-Based General Active Contours Energy

Let $\Omega \subset \mathbb{R}^2$ be the image domain and $\gamma : [0,1] \to \Omega$ be a regular curve with outward normal vector $\mathcal{N}$. Given a function $f : \Omega \to \mathbb{R}$ of interest, we consider the curve evolution scheme:

$$\frac{\partial \gamma}{\partial \tau} = f(\gamma) \mathcal{N}, \tag{11}$$

where τ denotes time. It is known that this curve evolution equation can be regarded as a gradient descent, thus a minimization procedure, for the following functional [35]

$$F(\gamma) = \int_K f(\mathbf{x}) \, d\mathbf{x}, \tag{12}$$

where $K \subset \Omega$ is the region inside the closed curve $\gamma := \partial K$. A complete active contour energy, involving a curve length penalization, can be defined as

$$E(\gamma) = \alpha F(\gamma) + \int_0^1 P(\gamma(t)) \|\dot{\gamma}(t)\| \, dt, \tag{13}$$

where P is an edge-based potential function, and $\alpha > 0$ is a balancing parameter.

3.2 Reformulation as Finsler Geodesic Energy

The goal of this section is to express the region-based active contour energy E in (13) as a pure geodesic contour energy. Suppose $\mathcal{V}_\perp : \Omega \to \mathbb{R}^2$ to be a continuously differentiable vector field defined over the domain Ω such that $\mathcal{V}_\perp$ satisfies the following divergence equation:

$$\nabla \cdot \mathcal{V}_\perp(\mathbf{x}) = \alpha f(\mathbf{x}), \quad \forall \mathbf{x} \in \Omega, \tag{14}$$

where f is the first order derivative function used in (12) and $\nabla \cdot \mathcal{V}_\perp(\mathbf{x})$ denotes the divergence value of a vector $\mathcal{V}_\perp(\mathbf{x})$. Letting M be the counter-clockwise rotation matrix with rotation

angle $\theta = \pi/2$, by divergence theorem, the regional energy (12) can be expressed as

$$\alpha F(\gamma) := \alpha \int_K f(\mathbf{x})d\mathbf{x} = \int_K \nabla \cdot \mathcal{V}_\perp(\mathbf{x})\, d\mathbf{x} \tag{15}$$

$$= \int_0^1 \langle \mathcal{V}_\perp(\gamma(t)), \mathcal{N}(t) \rangle \| \dot{\gamma}(t) \| \, dt \tag{16}$$

$$= \int_0^1 \langle M^{\mathrm{T}} \mathcal{V}_\perp(\gamma(t)), M^{\mathrm{T}} \mathcal{N}(t) \| \dot{\gamma}(t) \| \rangle \, dt \tag{17}$$

$$= \int_0^1 \langle \mathcal{V}(\gamma(t)), \dot{\gamma}(t) \rangle \, dt, \tag{18}$$

where $\mathcal{V} = M^{\mathrm{T}} \mathcal{V}_\perp$. Unit vector $\mathcal{N}$ is the outward normal vector of contour γ and $\dot{\gamma}$ is the tangent vector of γ in **clockwise** order. Indeed, $\mathcal{T} = M^{\mathrm{T}} \mathcal{N}$ is the tangent vector and

$$\dot{\gamma}(t) = \| \dot{\gamma}(t) \| \mathcal{T}(t) = \| \dot{\gamma}(t) \| M^{\mathrm{T}} \mathcal{N}(t), \quad \forall t \in [0,1].$$

One can introduce a Finsler metric $\mathcal{F} : \Omega \times \mathbb{R}^2 \to \mathbb{R}$:

$$\mathcal{F}(\mathbf{x}, \mathbf{u}) = P(\mathbf{x}) \| \mathbf{u} \| + \langle \mathcal{V}(\mathbf{x}), \mathbf{u} \rangle, \tag{19}$$

which is positive, thus well defined, provided one has the smallness condition (8):

$$\| \mathcal{V}(\mathbf{x}) \| < P(\mathbf{x}), \quad \forall \mathbf{x} \in \Omega. \tag{20}$$

In practice, it is difficult to satisfy the smallness condition (20). Assuming that $P(\mathbf{x}) \geq 1, \forall \mathbf{x} \in \Omega$, we make use of the following condition:

$$\| \mathcal{V}(\mathbf{x}) \| < \min_{\mathbf{y} \in \Omega} \{ P(\mathbf{y}) \} = 1, \quad \forall \mathbf{x} \in \Omega. \tag{21}$$

In view of $\mathcal{F}$ and (15), the energy E (13) is converted to the Finsler geodesic energy:

$$\mathcal{L}(\gamma) = \int_0^1 \mathcal{F}(\gamma(t), \dot{\gamma}(t)) dt. \tag{22}$$

3.3 Finsler Geodesics Evolution for Active Contours

In this section, we give the overview of the proposed Finsler geodesics evolution model by an iterative minimization scheme. Note that non-linear region energies can be approximated, at first order, by a linear region energy (12), which extends the scope of our method.

The basic idea is to seek a family of **clockwise** contours $\mathcal{C}_\tau : [0,1] \to \Omega$, $\tau \in \{0,1,\cdots\}$, which converge as $\tau \to \infty$ to the object boundary. The initialization of the proposed algorithm can be done by giving an initial contour $\mathcal{C}_0 : [0,1] \to \Omega$ involving a set of successive points

$$\Lambda_0 = \{ \mathcal{C}_0(t_i); t_i \in [0,1], i = 1,2,\cdots,m \}$$

in **clockwise order**. These points split $\mathcal{C}_0$ to m paths with same Euclidean curve length. Λ_0 can be chosen automatically or can be specified by user.

The first step of the proposed method, see line 1 of Algorithm 1, is to construct updated paths $\mathcal{C}_{\tau+1}$ by minimizing a geodesic energy $\mathcal{L}$ within a tubular neighborhood U of $\mathcal{C}_\tau$. Note

---

Algorithm 1 Minimization Scheme

Input: given contour $\mathcal{C}_0$ and its sampled points collection Λ_0.
Output: Final contour $\mathcal{C}$.
Initialization:
- Set $\Lambda \leftarrow \Lambda_0$ and $\tau \leftarrow 0$.
- Build the tubular neighbourhood region U according to $\mathcal{C}_0$.
- Update the metric $\mathcal{F}$= *UpdateFinslerMetric*$(\mathcal{C}_0, I, U)$

while $(d_H > \varepsilon)$
1: $[\mathcal{C}^*, \Lambda^*]$=*UpdateMinimalPaths*$(\mathcal{C}_\tau, \mathcal{F}, \Lambda, U)$.
2: Update neighbourhood U of $\mathcal{C}^*$.
3: Compute the Hausdorff distance d_H of paths $\mathcal{C}^*$ and $\mathcal{C}_\tau$.
4: $\tau \leftarrow \tau + 1$.
5: $\mathcal{C}_\tau \leftarrow \mathcal{C}^*$ and $\Lambda \leftarrow \Lambda^*$.
6: $\mathcal{F}$=*UpdateFinslerMetric*$(\mathcal{C}_\tau, I, U)$.

---

that both $\mathcal{L}$ and U depend on the previous paths $\mathcal{C}_\tau$. The tubular search region U should be sufficiently thin so as to avoid shortcuts.

The second step is to update the term f appearing in the region energy (12). (This is only required if (12) is used to approximate a more complex energy depending non-linearly on the region K.) Then the metric $\mathcal{F}$ can be updated as introduced in Section 3.5 below, which involves solving a linear system for computing the vector field $\mathcal{V}_\perp$. We repeat the mentioned two steps until the path $\mathcal{C}_\tau$ converges. The proposed algorithm can be found in Algorithm 1, where the functions *UpdateFinslerMetric* and *UpdateMinimalPaths* are detailed in Sections 3.4 and 3.5.

Construction of Tubular Neighbourhood U: The tubular neighbourhood region U of a curve $\mathcal{C}$ can be defined in terms of geodesic distance map $\mathcal{E}$ and a threshold value d:

$$U := \{\mathbf{x} \in \Omega; \mathcal{E}(\mathbf{x}) \le d\}, \tag{23}$$

where the geodesic distance map is computed by solving the following Eikonal Equation:

$$\begin{cases} \|\nabla \mathcal{E}(\mathbf{x})\| = \Psi(\mathbf{x}), & \forall \mathbf{x} \in \Omega \backslash \{\mathcal{C}\}, \\ \mathcal{E}(\mathbf{y}) = 0, & \forall \mathbf{y} \in \mathcal{C}. \end{cases}$$

The potential function Ψ is computed by using the region K inside the curve $\mathcal{C}$ and function f in (14). Specifically, for $\delta_1 \ge \delta_2 > 0$, one has

$$\Psi(\mathbf{x}) := \begin{cases} \delta_1, & \text{if } \mathbf{x} \in K \text{ and } f(\mathbf{x}) > 0, \\ \delta_1, & \text{if } \mathbf{x} \in K^c \text{ and } f(\mathbf{x}) < 0, \\ \delta_2, & \text{otherwise.} \end{cases} \tag{24}$$

3.4   Strategy for Finsler Minimal Paths Extraction

In this section, we present two methods for the function *UpdateMinimalPaths* based on different initialization ways. The first method is under the assumption that only an initial contour is provided. Another is based on the user-specified fixed points set. The goal of the function *UpdateMinimalPaths* is to minimize the geodesic energy $\mathcal{L}$ (22) with a fixed Finsler metric $\mathcal{F}$ and a tubular neighbourhood U.

Contour Initialization Scheme

Letting $\mathcal{C}$ be the given clockwise curve and Λ be its sampled points collection. our goal is to find a curve $\mathcal{C}^*$ minimizing $\mathcal{L}(\mathcal{C})$. For this purpose, we resample a collection of successive points from $\mathcal{C}$, denoted by Λ^*:

$$\Lambda^* := \{\mathbf{p}_i; \mathbf{p}_i \in \mathcal{C}, \mathbf{p}_i \notin \Lambda, i = 1, 2, \cdots, m\}. \tag{25}$$

We assume that points $\mathbf{p}_i$ are distributed evenly on $\mathcal{C}$ in a **clockwise** order. These points involved in Λ^* split the closed curve $\mathcal{C}$ into a set of paths $\mathcal{C}_i = \{\mathcal{C}_i; i = 1, 2, \cdots, m\}$. As a consequence, the geodesic energy $\mathcal{L}(\mathcal{C})$ in (22) can be expressed as:

$$\mathcal{L}(\mathcal{C}) = \sum_{i=1}^{m} \mathcal{L}(\mathcal{C}_i) = \sum_{i=1}^{m} \int_0^1 \mathcal{F}(\mathcal{C}_i(t), \dot{\mathcal{C}}_i(t)) dt. \tag{26}$$

For each curve $\mathcal{C}_i$, the tubular neighbourhood region $U_i \subseteq U$ is constructed by (23), where U is the neighbourhood region of $\mathcal{C}$. We extract the geodesic $\mathcal{C}_i^*$ between the pair of successive points $\mathcal{C}_i(0)$ and $\mathcal{C}_i(1)$, where $\mathcal{C}_i^*(0) = \mathcal{C}_i(0)$ and $\mathcal{C}_i^*(1) = \mathcal{C}_i(1)$. This is done by solving the Eikonal equation (9) with respect to the metric $\mathcal{F}$ inside U_i [□]. Then the curve $\mathcal{C}^*$ is concatenated by $\mathcal{C}_i^*$. Such a geodesic extraction scheme can be repeated by letting $\Lambda := \Lambda^*$ and $\mathcal{C} := \mathcal{C}^*$. Since $\mathcal{C}^*$ consists of a set of geodesics, one has $\mathcal{L}(\mathcal{C}) \leq \mathcal{L}(\mathcal{C}^*)$. When the number of repeating operation tends to ∞, $\mathcal{L}$ will converge to its minimum. This scheme can be stopped when the Hausdorff distance between $\mathcal{C}$ and $\mathcal{C}^*$ is small enough.

Fixed Points Initialization Scheme

If the points collection Λ^0 is provided by user and initially located in the object boundary exactly, we simply set $\Lambda^* := \Lambda_0$. The curve $\mathcal{C}^*$ is constructed in a same way as discussed above and no further iterations of the algorithm are needed since Λ^* is fixed, unless the tubular search region U was too small.

3.5 Computing the vector field $\mathcal{V}_\perp$ and Finsler Metric $\mathcal{F}$

The minimization procedure of $\mathcal{L}$ (22) is solved inside a neighbourhood U instead of the whole domain Ω. This means that we only require the vector field $\mathcal{V}^\perp$ defined over U. In order to satisfy the smallness condition (21), it is natural to select a solution to (14) minimizing an energy

$$\min \left\{ \int_U \|\mathcal{V}_\perp(\mathbf{x})\|^2 d\mathbf{x} \right\}, \quad s.t. \quad \nabla \cdot \mathcal{V}_\perp(\mathbf{x}) = \alpha f(\mathbf{x}), \quad \forall \mathbf{x} \in U. \tag{27}$$

Note that the solution to (27) can be expressed as $\mathcal{V}_\perp = \nabla \varphi$ where φ is the solution of the Poisson equation $\triangle \varphi = f$ over U with Neumann boundary conditions. Despite the rich regularity for solutions to elliptic PDEs, we could not find a result directly implying that the solution to (27) obeys the desired smallness condition (21). However, such a result can easily be established for a different solution to the divergence equation (14), given by convolution with an explicit kernel

$$\mathcal{V}_\perp(\mathbf{x}) = \frac{\alpha}{2\pi} \int_U \frac{\mathbf{x} - \mathbf{y}}{\|\mathbf{x} - \mathbf{y}\|^2} f(\mathbf{y}) d\mathbf{y}.$$

In that case one indeed obtains using Holder's inequality

$$\frac{2\pi}{\alpha}\|\mathcal{V}_\perp(\mathbf{x})\| \leq \|f\|_q \left(\int_U \frac{1}{\|\mathbf{x}-\mathbf{y}\|^p} d\mathbf{y} \right)^{\frac{1}{p}} \leq \|f\|_q \left(\int_{D_U} \frac{1}{\|\mathbf{x}-\mathbf{z}\|^p} d\mathbf{z} \right)^{\frac{1}{p}} = \eta A_U^\mu \|f\|_q, \quad (28)$$

where D_U is a disk centered around $\mathbf{x}$ and with the same area A_U as U. p, q are two positive constants obeying $1/p + 1/q = 1$ and $q > 2$. η is a constant and $\mu = \frac{1}{p} - \frac{1}{2} > 0$. $\|f\|_q$ is the L^q norm of f on U. The smallness condition is thus satisfied as soon as the area of U is sufficiently small.

Finsler Metric Construction

The vector field $\mathcal{V}_\perp$ solution to (27) depends on the neighbourhood U. In order to obtain a vector field obeying $\|\mathcal{V}_\perp\|_\infty < 1$, one choose a tubular neighbourhood U with small width hence a small area. On the other hand, U is regarded as the search space for the next evolutional curve as discussed in Section 3.4. A small U may therefore make the algorithm fall into undesirable local minimas of the geodesic energy $\mathcal{L}$. Thus we use two tricks to solve this issue. The first trick is to make the parameter $\alpha = 1/\|\mathcal{V}_\perp\|_\infty + \varepsilon$ (see (27)) where ε is a small positive constant.

In this paper, we make use of the second trick invoking a non-linear mapping increasing function $T : \mathbb{R}^+ \to (0,1)$ defined as $T(x) = 1 - \exp(-x), \forall x > 0$. Thus the new vector field $\bar{\mathcal{V}}$ can be expressed by

$$\bar{\mathcal{V}}(\mathbf{x}) = T(\|\mathcal{V}_\perp(\mathbf{x})\|) \frac{M^{-1}\mathcal{V}_\perp(\mathbf{x})}{\|\mathcal{V}_\perp(\mathbf{x})\|}, \quad \forall \mathbf{x} \in \Omega. \quad (29)$$

where the smallness condition (21) will be immediately satisfied and M is the counterclockwise rotation matrix with rotation angle $\theta = \pi/2$. Based on the vector field $\bar{\mathcal{V}}$, the new Finsler metric $\bar{\mathcal{F}}$ is defined by (19) with $\mathcal{V} := \bar{\mathcal{V}}$, and the corresponding geodesic energy $\bar{\mathcal{L}}$ is defined by (22) with $\mathcal{F} := \bar{\mathcal{F}}$.

The minimization of E (13) is transferred to the minimization of $\bar{\mathcal{L}}$. Note that since in general we induce $\bar{\mathcal{L}}$ with a nonlinear mapping T, there is in fact slight difference in the minimization problems and the results show that our geodesic method is very efficient and robust. Two points guarantee that using the non-linear mapping T is reasonable:

• The minimization of E in (15) is relevant to both the directions of γ and the norm of $\mathcal{V}$, i.e., minimizing E is to find a path γ, for which the direction $\gamma'(t)$ for each $t \in [0, 1]$ should be as opposite to $\mathcal{V}(\gamma(t))$ as possible and the norm $\|\mathcal{V}(\gamma(t))\|$ should be as large as possible, giving the relevance between the minimization problems of E and $\bar{\mathcal{L}}$. Introducing the nonlinear mapping T will not modify both goals of the minimization problems.

• When the Finsler geodesics evolution scheme as discussed in Algorithm 1 tends to stabilize, one can reduce the width of tubular neighbourhood U. Thus $T(\|\mathcal{V}\|) \approx \|\mathcal{V}\|$ as $\|\mathcal{V}\|$ is small. Moreover, We experimentally observe that near the centreline of U, the values of $\|\mathcal{V}\|$ will vanish or become very small, leading to a good approximation of $\mathcal{V}$ by $\bar{\mathcal{V}}$.

4 Experiments

In Fig. 1, we show the course of the proposed contour evolution method using contour initialization scheme as described in Section 3.4. The function f in (14) is obtained by using the
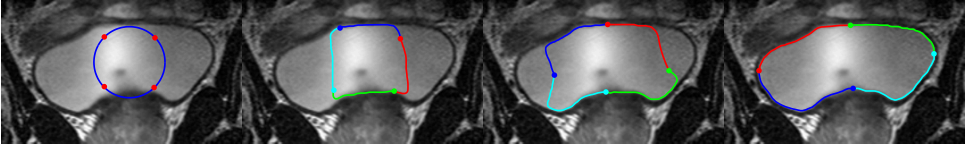
Figure 1: Steps of the proposed algorithm using contour initialization scheme. **Column 1** The initial contour and sampled control points are demonstrated. **Columns 2-3** Intermediate curve evolution results. **Column 4** Final segmentation result.
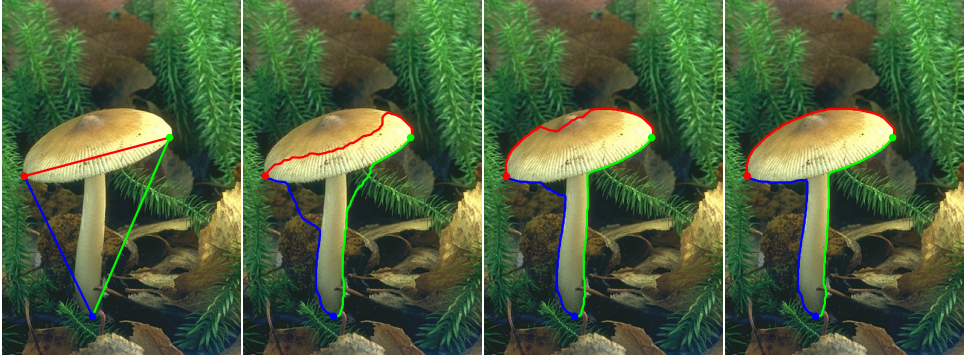

Figure 2: Steps of the proposed algorithm using fixed points initialization scheme. **Column 1** demonstrates the fixed control points and the initial contour linking these control points. **Columns 2-4** show the geodesic evolution results.

Figure 3: Comparative segmentation results on natural images. **Column 1** demonstrate the initializations. **Column 2** shows the segmentation results from the LBF model. **Column 3** shows the segmentation results from the proposed model with fixed points scheme.

LBF energy, i.e. f is the Euler-Lagrange equation of the LBF energy functional [21]. We set $P \equiv 1$ in this experiment. In column 1 of Fig. 1, red dots indicate successive control points

Figure 4: Segmentation results using the proposed model with contour initialization scheme.

sampled from the initial contour (blue curve). Each pair of successive control points leads a geodesic, indicated by the color same to its corresponding initial source point as shown in columns 2-4. Columns 2-3 demonstrate the intermediate segmentation results and column 4 presents the final stable contour.

In Fig. 2, we show the course of the proposed model using the fixed point initialization scheme. Column 1 demonstrates the fixed control points denoted by coloured dots, where the initial closed contour is obtained by linking those successive control points. Columns 2-3 are the intermediate segmentation results and column 4 is the final result. In this experiment, our model requires only 3 steps to converge to the expected boundary. The function f is obtained using the CV energy [10] and potential P depends on gradient magnitude.

In Fig. 3 we show the comparative results from the LBF model with distance preserved level set implementation [21, 22] and the proposed model with fixed points initializations (red dots are the user provided points), demonstrated in columns 2 and 3 respectively. The initializations are shown in column 1. Thanks to the robust minima searching scheme of the proposed model, the results in column 3 can catch the desired boundaries. In contrast, the results from the LBF model fall into the false local minimas. In this experiment, we use LBF energy to derivate f (see (11)) for fair comparisons and set $P \equiv 1$.

In Fig. 4, we show segmentation results from the proposed model using contour initialization scheme. In this figure, green dash curves are the initial contours and blue curves are the final segmentation results. The data function f (11) are obtained from the LBF energy [21] and set $P \equiv 1$.

5 Conclusion

In this paper, we show the possibilities of evolving the Eikonal equation-based minimal paths for region-based image segmentation. The minimal paths are based on a Finsler metric that is obtained by applying a non-linear mapping to a vector field that is treated as the solution of a linear constraint minimization problem. We design two geodesics extraction schemes to obtain the closed contour in each curve evolution iteration within a tubular neighbourhood region of the previous closed contour. Experimental results show that the proposed model indeed obtains promising segmentation results.

Acknowledgement

References

[1] V. Appia and A. Yezzi. Active geodesics: Region-based active contour segmentation with a global edge-based constraint. In *Proceedings of IEEE International Conference on Computer Vision (ICCV 2011)*, pages 1975–1980, 2011.

[2] Ben Appleton and Hugues Talbot. Globally optimal geodesic active contours. *Journal of Mathematical Imaging and Vision*, 23(1):67–86, 2005.

[3] Erik J Bekkers, Remco Duits, Alexey Mashtakov, and Gonzalo R Sanguinetti. A pde approach to data-driven sub-riemannian geodesics in se (2). *SIAM Journal on Imaging Sciences*, 8(4):2740–2770, 2015.

[4] F. Benmansour and L. D. Cohen. Fast object segmentation by growing minimal paths from a single point on 2D or 3D images. *Journal of Mathematical Imaging and Vision*, 33(2):209–221, 2009.

[5] F. Benmansour and L. D. Cohen. Tubular Structure Segmentation Based on Minimal Path Method and Anisotropic Enhancement. *International Journal of Computer Vision*, 92(2):192–210, 2011.

[6] Luca Bertelli, Baris Sumengen, BS Manjunath, and Frédéric Gibou. A variational framework for multiregion pairwise-similarity-based image segmentation. *IEEE Trans. on Pattern Analysis and Machine Intelligence*, 30(8):1400–1414, 2008.

[7] S. Bougleux, G. Peyré, and L. Cohen. Anisotropic Geodesics for Perceptual Grouping and Domain Meshing. In *Proceedings of European Conference on Computer Vision (ECCV 2008). Springer Berlin Heidelberg*, pages 129–142, 2008.

[8] Thomas Brox and Daniel Cremers. On local region models and a statistical interpretation of the piecewise smooth Mumford-Shah functional. *International Journal of Computer Vision*, 84(2):184–193, 2009.

[9] V. Caselles, R. Kimmel, and G. Sapiro. Geodesic active contours. *International Journal of Computer Vision*, 22(1):61–79, 1997.

[10] Tony F Chan and Luminita A Vese. Active contours without edges. *IEEE Trans. on Image Processing*, 10(2):266–277, 2001.

[11] D. Chen and L. D. Cohen. Piecewise Geodesics for Vessel Centreline Extraction and Boundary Delineation with Application to Retina Segmentation. In *Proceedings of Scale Space and Variational Methods in Computer Vision (SSVM 2015)*, pages 270–281, 2015.

[12] Da Chen and Laurent D Cohen. Interactive retinal vessel centreline extraction and boundary delineation using anisotropic fast marching and intensities consistency. In *Proceedings of EMBC 2015*, pages 4347–4350, 2015.

[13] Da Chen, Laurent D Cohen, and J-M Mirebeau. Vessel extraction using anisotropic minimal paths and path score. In *Proceedings of IEEE International Conference on Image Processing (ICIP 2014)*, pages 1570–1574, 2014.

[14] Da Chen, Jean-Marie Mirebeau, and Laurent D Cohen. Global Minimum for Curvature Penalized Minimal Path Method. In *Proceedings of the British Machine Vision Conference (BMVC 2015)*, pages 86.1–86.12, 2015.

[15] L. D. Cohen. On active contour models and balloons. *CVGIP: Image understanding*, 53(2):211–218, 1991.

[16] L. D. Cohen and R. Kimmel. Global minimum for active contour models: A minimal path approach. *International Journal of Computer Vision*, 24(1):57–78, 1997.

[17] Anastasia Dubrovina-Karni, Guy Rosman, and Ron Kimmel. Multi-region active contours with a single level set function. *IEEE Trans. on Pattern Analysis and Machine Intelligence*, 37(8):1585–1601, 2015.

[18] Miyoun Jung, Gabriel Peyré, and Laurent D Cohen. Nonlocal active contours. *SIAM Journal on Imaging Sciences*, 5(3):1022–1054, 2012.

[19] M. Kass, A. Witkin, and D. Terzopoulos. Snakes: Active contour models. *International Journal of Computer Vision*, 1(4):321–331, 1988.

[20] Shawn Lankton and Allen Tannenbaum. Localizing region-based active contours. *IEEE Trans. on Image Processing*, 17(11):2029–2039, 2008.

[21] Chunming Li, Chiu-Yen Kao, John C Gore, and Zhaohua Ding. Minimization of region-scalable fitting energy for image segmentation. *IEEE Trans. on Image Processing*, 17(10):1940–1949, 2008.

[22] Chunming Li, Chenyang Xu, Changfeng Gui, and Martin D Fox. Distance regularized level set evolution and its application to image segmentation. *IEEE Transactions on Image Processing*, 19(12):3243–3254, 2010.

[23] J. Melonakos, E. Pichon, S. Angenent, and A. Tannenbaum. Finsler active contours. *IEEE Trans. on Pattern Analysis and Machine Intelligence*, 30(3):412–423, 2008.

[24] J. Mille, S. Bougleux, and L. Cohen. Combination of piecewise-geodesic paths for interactive segmentation. *International Journal of Computer Vision*, 112(1):1–22, 2014.

[25] Jean-Marie Mirebeau. Efficient fast marching with Finsler metrics. *Numerische Mathematik*, 126(3):515–557, 2014.

[26] David Mumford and Jayant Shah. Optimal approximations by piecewise smooth functions and associated variational problems. *Communications on pure and applied mathematics*, 42(5):577–685, 1989.

[27] S. Osher and J. A. Sethian. Fronts propagating with curvature-dependent speed: algorithms based on Hamilton-Jacobi formulations. *Journal of computational physics*, 79(1):12–49, 1988.

[28] J. A. Sethian. Fast marching methods. *SIAM Review*, 41(2):199–235, 1999.

[29] Baris Sumengen and BS Manjunath. Graph partitioning active contours (GPAC) for image segmentation. *IEEE Trans. on Pattern Analysis and Machine Intelligence*, 28(4):509–521, 2006.

[30] Andy Tsai, Anthony Yezzi Jr, and Alan S Willsky. Curve evolution implementation of the Mumford-Shah functional for image segmentation, denoising, interpolation, and magnification. *IEEE Trans. on Image Processing*, 10(8):1169–1186, 2001.

[31] Luminita A Vese and Tony F Chan. A multiphase level set framework for image segmentation using the Mumford and Shah model. *International Journal of Computer Vision*, 50(3):271–293, 2002.

[32] Xianghua Xie and Majid Mirmehdi. MAC: Magnetostatic active contour model. *IEEE Trans. on Pattern Analysis and Machine Intelligence*, 30(4):632–646, 2008.

[33] C. Xu and J. L Prince. Snakes, shapes, and gradient vector flow. *IEEE Trans. on Image Processing*, 7(3):359–369, 1998.

[34] Hong-Kai Zhao, Tony Chan, Barry Merriman, and Stanley Osher. A variational level set approach to multiphase motion. *Journal of computational physics*, 127(1):179–195, 1996.

[35] Song Chun Zhu and Alan Yuille. Region competition: Unifying snakes, region growing, and Bayes/MDL for multiband image segmentation. *IEEE Trans. on Pattern Analysis and Machine Intelligence*, 18(9):884–900, 1996.